Photocatalytic Treatment of Different Types of High–Concentration Ammonia Wastewater by Cu/TiO_2 Film and its Mechanism Study

Jianpei Feng
Harbin Institute of Technology
Guan Zhang (zhangguan@hit.edu.cn)
Harbin Institute of Technology https://orcid.org/0000-0001-7089-7536
Xiaolei Zhang
Harbin Institute of Technology
Ji Li
Harbin Institute of Technology

Research Article

Keywords: Cu/TiO2 films, photocatalytic oxidation, high concentration ammonia removal, N2 formation, wastewater treatment

Posted Date: September 2nd, 2021

DOI: https://doi.org/10.21203/rs.3.rs-688668/v1

Abstract

Photocatalytic oxidation of ammonia in wastewater has been abundantly investigated in lab – scale, but there are still many issues to be solved towards practical application. Herein, we have immobilized Cu/TiO_2 photocatalyst on different solid substrates in order to practically utilize and recycle the photocatalyst during wastewater treatment, on the basis of exploring the effects of different influencing factors such as pH, temperature and salinity on the photocatalytic oxidation of ammonia in this work. The performance of Cu/TiO_2 films was evaluated by circulated treatment of different types of wastewater including high salinity ammonia wastewater, copper – ammonia wastewater and liquid – ammonia mercerization wastewater. The characters of wastewater matrices significantly influence the performance for ammonia oxidation. Different from the slurry test of photocatalyst power that operated in a closed reactor, it is importantly found that oxygen in air plays significant role in photocatalytic oxidation of ammonia into dinitrogen in the aerobic oxidation process, when the Cu/TiO_2 films were employed. The possible oxidation mechanism has been proposed to elucidate the ammonia oxidation process.

Introduction

There are a variety of methods to remove ammonia from contaminated wastewater, including ion exchange, breakpoint chlorination, adsorption, biological treatment, chemical oxidation, membrane separation, and advanced oxidation processes (Charrois and Hrudey 2007; Song et al. 2019; Wang et al. 2014; Zeng et al. 2019). Generally, sewage plants use cost – effective biological methods to remove ammonia nitrogen in sewage through nitrification and denitrification. In this microbial – based process, NH_4^+/NH_3 is converted to NO_2^- and (or) NO_3^- under aerobic condition, and then reduced to N_2 under anoxic condition (Fei et al. 2020). However, some wastewater with high – concentration ammonia is not suitable for biochemical treatment due to the limited microbial activities under specific condition. For example, high salinity ammonia nitrogen wastewater (NaCl and Na_2SO_4) will inhibit the microbial activity of the biochemical system and reduce the abundance and diversity of microbial communities, especially high concentrations of Cl^- will reduce the biodegradation efficiency of ammonia nitrogen (Chen et al. 2018; Feng et al. 2020; Hong et al. 2013; Li et al. 2020; She et al. 2016). Copper – ammonia complex polluted wastewater not only has a high – concentration ammonia and high pH, but also contains copper ammonia complex ($Cu(NH_3)_4^{2+}$), which are very stable and can poison microorganisms, so the copper ions in water need to be removed before subsequent biochemical treatment (Chai et al. 2017; Dai et al. 2013; Peng et al. 2017; Yang and Kocherginsky 2007). The high pH, high – concentration ammonia and low C/N ratio in liquid – ammonia mercerization wastewater produced in the textile industry strongly inhibit biological activity (RigoniStern et al. 1996), which results in high cost of biological treatment through complete nitrification and denitrification (Zheng et al. 2020).

Among the different physicochemical treatment approaches, heterogeneous photocatalytic oxidation (PCO) could be considered for removing high – concentration ammonia in wastewater and there are many literature research about this. The final products of photocatalytic conversion of ammonia by TiO_2 under

the UV irradiation are mainly N_2 and NO_3^-, depending on the cocatalyst on TiO_2. Some studies have shown that loading precious metals on TiO_2 can significantly improve the photocatalytic activity (Takata et al. 2019). For example, Pt/TiO_2 photocatalyst shows significantly improved activity for ammonia oxidation and N_2 selectivity (Takata et al. 2019). We also found that 0.3 wt% Cu loaded TiO_2 photocatalyst shows comparable photocatalytic activity with Pt/TiO_2 for oxidizing low concentration of ammonia, but exhibits much higher photocatalytic activity for oxidizing high concentration of ammonia, primarily ascribed to the Cu metal mediated complexation effect (Feng et al. 2021). In order to practically employ the photocatalyst powder, immobilization of powder onto solid substrate or deposition onto a film is necessary to improve its stability and recyclability (Zhou et al. 2019). In this work, in order to test the Cu/TiO_2 photocatalyst for the treatment of wastewater with high – concentration ammonia, the experimental influencing factors, oxidation efficiency and products, photocatalyst immobilization methods and treatment of different types of wastewater were explored.

Materials And Methods

Preparation of Cu/TiO_2 photocatalyst film

According to our previous work, the copper (0.325 wt%) – loaded TiO_2 (P25) was obtained by photoreduction deposition. The Cu/TiO_2 photocatalyst film was prepared by the drip coating method. Titanium sheets, copper sheets, glass, and ITO conductive glass were selected as the supports of the photocatalyst film. The supports were immersed in deionized water for ultrasonic cleaning for 20 minutes and dried. An appropriate amount of catalyst powder was mixed with ethanol to form a drop coating slurry (100 mg/mL), and ultrasonically dispersed for 60 minutes. The slurry was slowly dropped on the horizontally placed support until the slurry evenly covers its surface. Finally, it was dried at 60 ^oC for 24 h to form the homogeneously dispersed photocatalyst film.

Photocatalytic oxidation of ammonia nitrogen

Influencing factors of slurry experiments

The slurry experiments of photocatalytic degradation of ammonia nitrogen under UV light irradiation (Xe lamp (PLS – SEX300)) in the presence of photocatalyst powder was carried out in a quartz reactor coated with a quartz glass from top to avoid ammonia valorization. The pH of the solution was adjusted by using 1.0 M NaOH and 1.0 M HCl. The reaction temperature was maintained at about 20 ^oC by a cryostat. The sample was taken out from the sampling port and centrifuged at 14000 rpm for 15 minutes so that the supernatant can be obtained to test.

Activity test of photocatalyst film

As shown in Fig. 1, the photocatalytic activity of film was tested in a water – circulated condition with UV light irradiation from the top of the photocatalyst film. The prepared photocatalyst film was placed on the

bottom of an open reactor, and the water circulated between the wastewater tank and the open reactor to allow the water flow on the surface of the photocatalyst film. Three typical high − concentration ammonia nitrogen wastewaters are selected to investigate the performance of the photocatalyst film. The simulated wastewater characters are shown as follows. High salinity ammonia nitrogen wastewater: [NH_3 − N] = 500 mg/L, [SO_4^{2-}] = 10000 mg/L and [Cl^-] = 10000 mg/L. Copper − ammonia complex wastewater: [NH_3 − N] = 500 mg/L, and [Cu^{2+}] = 200 mg/L. Liquid − ammonia mercerization wastewater: [NH_3 − N] = 500 mg/L, and [COD_{Cr}] = 200 mg/L (sodium acetate as the donor).

Detection and analysis methods

Surface chemical composition of the photocatalyst and valence state of the copper were analyzed by the X − ray photoelectron spectroscopy (XPS, PHI 5000 VersaProbe II). The reaction liquid sample was taken out from the sampling port at regular intervals to detect the concentration of ammonia nitrogen (NH_4^+/NH_3 − N), nitrite nitrogen (NO_2^-−N), nitrate nitrogen (NO_3^-−N) and copper ions. The concentration of ammonia nitrogen, nitrite nitrogen and nitrate nitrogen in the solution is detected by spectrophotometry with an ultraviolet − visible spectrophotometer (Agilent, Cary 5000). The copper ion concentration was quantitatively analyzed by inductively coupled plasma emission spectrometer (ICP − OES, Optima 8000).

Results And Analysis

Effect of the initial pH on the removal of ammonia nitrogen

The photocatalytic conversion of ammonia nitrogen (500 mg/L) in aqueous solution with different initial pH is shown in Fig. 2. The initial pH greatly affected the photocatalytic oxidation of ammonia nitrogen. As shown in Fig. 2a, the ammonia removal rate was improved with the increase of the initial pH, which reaches an optimum pH value of 10.0 − 11.0. However, when the pH is 7.0, the ammonia nitrogen concentration is basically unchanged. It is known that when the solution is acidic and neutral, the ammonia nitrogen exists in the form of NH_4^+ which hydroxyl radicals generated by photocatalysis cannot easily attack (Lee et al. 2002; Yao et al. 2020). Fig. S1 shows that under different pH conditions, the process of photocatalytic ammonia nitrogen is fitted with the first − order kinetic reaction process. The pH not only influences on the conversion of ammonia nitrogen, but also the oxidation products. It can be seen from Fig. 2b that when the pH increases from 7.0 to 10.0, the amount of gaseous − N species generated increases. However, the conversion rate of ammonia nitrogen into N_2 and other gases decreases with the increase of pH. Table S1 shows that the gas conversion rate is 94.0% under the pH = 8.0 and the gas conversion rate drops to 61.2% under the pH = 11.0. The reason is probably that the increase in pH facilitates generation of hydroxyl radicals ●OH, which mainly produces nitrite and nitrate nitrogen. According to the previous work (Feng et al. 2021), the key to generation of gaseous − N species is superoxide radical ●O_2^-. As the pH increases, superoxide radical ●O_2^- was gradually depleted due to the limited dissolved oxygen in the closed reaction system. The generated ionic species were also

monitored. As shown in Fig. 2c and Fig. 2d, nitrite ions were found as the major products and nitrate ions are negligible. With the increase of pH, more nitrite ions were produced in 6 h reaction.

Effect of temperature on the removal of ammonia

The photocatalytic conversion of ammonia nitrogen in aqueous solution with different temperatures is shown in Fig. 3. As shown in Fig. 3a, the removal efficiency of ammonia nitrogen does not change significantly when the temperature rises from 20 ^{o}C to 30 ^{o}C. However, when the temperature is increased to 40 ^{o}C and 50 ^{o}C, the removal efficiency of ammonia nitrogen is improved. Fig. S2 shows that under different temperature conditions, the process of photocatalytic ammonia nitrogen is consistent with the first – order kinetic reaction process. When the temperature is greater than 30 ^{o}C, the reaction rate increases with the increase of the reaction temperature. Therefore, it can be considered that the increase in temperature promotes the reaction rate mainly because of the increase in the number of molecular collisions, rather than the increase in the number of thermally activated molecules. As the reaction temperature increases, the amount of ammonia nitrogen converted into N_2 and other gases gradually increases, probably due to the reduced gas solubility in water accelerates the release of gaseous products into gas phase.

According to the data in Table S1, the Arrhenius Eq. (1) can be used to calculate the activation energy of photocatalytic ammonia nitrogen (Jung and Kruse 2017).

$$\ln\left(\frac{k_2}{k_1}\right) = \frac{-E_a}{R}\left(\frac{1}{T_2} - \frac{1}{T_1}\right) \qquad (1)$$

In the formula, k is the reaction rate constant at temperature T (h^{-1}), E_a is the activation energy of the reaction (J/mol), R is the molar gas constant (J/mol·K), and T is the absolute temperature (K). According to the Arrhenius Eq. (1), with $\ln(k_2/k_1)$ as the ordinate and $(1/T_2 - 1/T_1)$ as the abscissa, using the least squares method to fit, the slope $-E_a/R$ can be obtained, and the activation energy of the reaction is finally calculated to be 8.421 kJ/mol.

Effect of the high salinity on the removal of ammonia nitrogen

Generally, industrial wastewater with high concentration of ammonia nitrogen has a high salinity. Therefore, the effect of excessive Cl^- and SO_4^{2-} on the photocatalytic oxidation of ammonia nitrogen was investigated. It can be seen from Fig. 4a that the removal of ammonia nitrogen is basically not affected by the high concentration of SO_4^{2-}. Under alkaline conditions, part of SO_4^{2-} could be converted into sulfate radicals ($SO_4^{\bullet-}$) by photogenerated $^{\bullet}$OH (Wang et al. 2021). Although high concentration of SO_4^{2-} consumes part of $^{\bullet}$OH, $SO_4^{\bullet-}$ has a higher oxidation – reduction potential (E_0 = 2.5 – 3.1 eV), and its oxidation capacity is equivalent to $^{\bullet}$OH (E_0 = 2.8 eV) (Song et al. 2019; Wang et al. 2019; Wang et al. 2019). Therefore, the high concentration of SO_4^{2-} basically does not affect the removal rate of ammonia

nitrogen. As shown from Fig. 4b, under the condition of high concentration of Cl^-, the removal effect of ammonia nitrogen is obviously suppressed and as the concentration of Cl^- increases, the removal rate of ammonia nitrogen gradually decreases. The reason may be that Cl^- has the ability to scavenge $^{\bullet}OH$, which convert part of Cl^- into chlorine radical $Cl^{\bullet}$ (E_0 = 2.4 eV) that can not efficiently degrade ammonia nitrogen directly, thereby inhibiting the removal rate of ammonia nitrogen (Han et al. 2021; Liou and Dodd 2021).

Treatment of wastewater by photocatalyst film

The Cu/TiO_2 photocatalyst powder was immobilized onto some solid substrates including titanium sheet, copper sheet, glass and ITO conductive glass. Figure 5a shows that the removal rate of ammonia nitrogen on glass substrate is the highest. In contrast, the efficiencies of photocatalytic oxidation of ammonia using titanium sheet, copper sheet and ITO supported photocatalytic films are relatively lower. Unlike the slurry tests in the closed reactor, the circulated film test system is open to the air, which is benefit for O_2 supply and improved mass transfer between aqueous and gaseous phases. It can be seen from Fig. 5b and Fig. S3 that only a small part of NH_3 is converted into NO_2^- and NO_3^-, and most of NH_3 is removed in the form of gaseous species. This is because superoxide radicals $\bullet O_2^-$ are proposed as the key oxidant to gas production (Feng et al. 2021), and the increased supply of oxygen in the open reactor system will increase the superoxide radicals $\bullet O_2^-$, and thus N_2 production will be increased.

The flow rate of circulated water on the surface of catalyst film has strong influence on its removal efficiency of ammonia nitrogen and catalyst stability. It can be seen from Fig. 6a and Fig. S4 – S6 that when the flow rate is 40 mL/min, the morphology of Cu/TiO_2@Glass before and after the photocatalytic reaction is basically unchanged, and the removal efficiency of ammonia nitrogen is the highest. When the flow rate increases, the catalyst film on the glass surface is damaged due to the excessive surface velocity, which leads to the weakening of the photocatalytic efficiency. However, when the flow rate decreases, the catalyst film on the glass surface is also damaged. The reason may be that the residence time of the solution on the surface of the catalyst film increases, and anions tend to accumulate on the surface of TiO_2 and destroy the bonding structure of TiO_2/SiO_2, thereby reducing the removal rate of ammonia (Levchuk et al. 2019). Therefore, the flow rate 40 mL/min was selected for subsequent experiments.

The circulated treatment of different types of high – concentration ammonia wastewater by Cu/TiO_2@Glass was investigated. In the control experiment (Fig. 7a), the ammonia was rapidly removed in the first hour, and then the oxidation rate gets slower. Because solution pH gradually decreases along with the ammonia removal, the photocatalytic oxidation of NH_4^+ in acidic or neutral condition is inhibited. Compared with Fig. 7a, the removal of ammonia in high salinity wastewater decreased significantly (Fig. 7b), the ammonia no longer drops after 4 h and about 165 mg/L of NH_3 – N can be removed finally. The reason is that excessive Cl^- consumes the h^+ and $^{\bullet}OH$ on the surface of the photocatalyst film, resulting in a decrease of photocatalytic oxidation efficiency (Wang et al. 2021). Figure 7c shows that the NH_3 – N

in the copper – ammonia complex wastewater no longer drops after 2 h and about 160 mg/L of NH_3 – N can be removed. The reason is that copper ions play a role in capturing e^- in the photocatalytic process, inhibiting the generation of $\bullet O_2^-$, resulting in a decrease of photocatalytic oxidation efficiency. However, Cu^{2+} ions in water can be reduced to Cu^+ or Cu depositing on photocatalyst film by the photogenerated electrons, which can be considered as simultaneous removal of NH_3 – N and Cu^{2+} according to the Fig. S7. Figure 7d shows that the NH_3 – N in the liquid – ammonia mercerization wastewater was slowly removed during 6 h reaction and about 135 mg/L of /NH_3 – N can be removed finally, since the organic matters in liquid – ammonia mercerization wastewater consume the h^+ and $\bullet OH$ produced on the surface of the photocatalyst film.

To investigate the stability of Cu/TiO_2@Glass during treatment of different wastewater, the experiments were repeated five times and the removal rates were shown in Fig. 8a. Cu/TiO_2@Glass film before and after the reaction was weighed, and the mass change was calculated as shown in Fig. 8b. For high salinity ammonia wastewater, as the number of reuses of photocatalyst film increases, the removal rate of NH_4^+/NH_3 – N gradually decreases and it is dropped by about 6% after five repeated experiments. In addition, the mass of photocatalyst film is continuously decreased because the excessive anions damages the surface structure of the film. Regarding the liquid – ammonia mercerization wastewater, although the organic matter has a greater inhibitory effect on the removal efficiency of NH_3 – N, the removal rate was only dropped by about 1.5% after five repeated experiments, indicating that organic matter has a small impact on the reusability of Cu/TiO_2@Glass. For copper – ammonia wastewater, as the number of reuses of Cu/TiO_2@Glass increases, the removal rate of NH_3 – N increases unpredictably. The removal of NH_3 – N increased from 56.6–67.7% during the first three cycles and then slightly decreased, but the removal rate is still higher than that of the first photocatalytic process. Besides, as the number of reuses increases, the mass of Cu/TiO_2@Glass continues to increase, because copper ions in the solution are continuously reduced and deposited on the surface of photocatalyst film. The deposited Cu species could be work as cocatalyst to enhance the photocatalytic performance (Mingmongkol et al. 2021).

Mechanism of photocatalytic conversion of ammonia

There are many pathways involved for photocatalytic oxidation of ammonia on Cu/TiO_2 as illustrated in Fig. 9. In the closed reactor condition, it has been proposed that $\bullet OH$, h^+ and $\bullet O_2^-$ are main oxidants for ammonia conversion, in which $\bullet O_2^-$ radical strongly influences the gaseous products (pathway I). However, due to the depletion of dissolved O_2 content, the reactions prefer to further proceed via pathways II and III, thus the conversion rate and selectivity to N_2 gradually decreases. In contrast, in the open system, the NH_3 abatement resulting from both the large portion of volatilization and photocatalytic oxidation would decrease the pH of the solution gradually, so that the reaction driven by $\bullet OH$ (pathway II and III) are limited. Moreover, due to the continuous supply of O_2 within 6 hours, the ammonia conversion driven by $\bullet O_2^-$ (pathway I) would be proceeded continuously, and the selective oxidation to gaseous

products was enhanced as shown in Fig. 9. It can be found that no matter what kind of Cu/TiO_2 films used in the open system, the removal of ammonia and the selectivity of gaseous products are higher than those of Cu/TiO_2 powder in the closed reactor, which further demonstrates the role of dissolved O_2 in the ammonia conversion.

Conclusions

The influencing factors such as pH, temperature and salinity strongly influence the photocatalytic oxidation of ammonia by Cu/TiO_2 photocatalyst. The results showed that the optimal initial pH is 10.0 under the high – concentration ammonia condition. After 6 hours, about 140 mg/L NH_4^+/NH_3 – N can be removed, of which 65.6% of ammonia was converted into N_2 and other gases. Increasing reaction temperature over 40 ^oC can markedly improve the photocatalytic oxidation efficiency. Excessive SO_4^{2-} (50000 mg/L) did not affect the removal effect of ammonia, but excessive Cl^- (50000 mg/L) inhibited the removal effect of ammonia. Furthermore, it was found that Cu/TiO_2 particles have strong affinity with glass substrate as the Cu/TiO_2@Glass film provides good stability compared to other solid supports during multiple repeated tests. In addition, the photocatalytic performance of Cu/TiO_2@Glass film, was excellent for treating different types of wastewater including high salinity ammonia wastewater, copper – ammonia wastewater and liquid – ammonia mercerization wastewater due to the continuous oxygen input from air, the improved photons absorption efficiency and strong stability. More importantly, the photocatalytic oxidation performance of Cu/TiO_2 film was superior to that of the Cu/TiO_2 powder, highlighting the advantages of Cu/TiO_2 film for practical application.

Declarations

Supplementary Information

The online version contains supplementary material available at http://doi.org/xx/

CRediT author statement

Jianpei Feng: Methodology, Investigation, Data analysis. **Guan Zhang**, Supervision, Writing, Funding acquisition. **Xiaolei Zhang**, Supervision, Funding acquisition. **Ji Li**, Supervision, Resources.

Data availability

All data generated or analyzed during this study are included in this published article and supplementary information files.

Acknowledgments

The authors thank the financial supports from NSFC (no. 51978197), the Shenzhen Science and Technology Innovation Commission (Grant No. JCYJ20180306171722756, JCYJ20180306172051662) and Pearl River talent plan (Young Scholar) of Guangdong Province.

Ethics approval and consent to participate

Not applicable

Consent for publication

Not applicable

Declaration of competing interest

The authors declare that there is no other interests or relationships that could have appeared to influence the work reported in this paper.

References

1. Chai L, Peng C, Min X, Tang C, Song Y, Zhang Y, Zhang J, Ali M (2017) Two–sectional struvite formation process for enhanced treatment of copper–ammonia complex wastewater. T Nonferr Metal Soc 27: 457–466. http://doi.org/10.1016/S1003–6326(17)60052–9
2. Charrois JWA, Hrudey SE (2007) Breakpoint chlorination and free–chlorine contact time: Implications for drinking water N–nitrosodimethylamine concentrations. Water Res 41: 674–682. http://doi.org/10.1016/j.watres.2006.07.031
3. Chen Y, He H, Liu H, Li H, Zeng G, Xia X, Yang C (2018) Effect of salinity on removal performance and activated sludge characteristics in sequencing batch reactors. Bioresource Technol 249: 890–899. http://doi.org/10.1016/j.biortech.2017.10.092
4. Dai M, Li J, Kang B, Ren C, Chang S, Dai Y (2013) Magnetic nanoparticle decorated multi–walled carbon nanotubes for removing copper ammonia complex from water. J Nanosci Nanotechno 13: 1927–1930. http://doi.org/10.1166/jnn.2013.7105
5. Fei X, Sun S, He S, Huang J, Zhou W (2020) Application of a novel two–stage biofiltration system for simulated brackish aquaculture wastewater treatment. Environ Sci Pollut R 27: 636–646. http://doi.org/10.1007/s11356–019–06969–z
6. Feng J, Zhang X, Zhang G, Li J, Song W, Xu Z (2021) Improved photocatalytic conversion of high–concentration ammonia in water by low–cost Cu/TiO_2 and its mechanism study. Chemosphere

274: 129689. http://doi.org/10.1016/j.chemosphere.2021.129689

7. Feng L, Luo Y, Yang J, Sun J (2020) Nitrogen removal characteristics in a biofilm system for recirculating aquaculture wastewater treatment under high–salinity conditions and oligotrophic stress. J Environ Eng 146:04020057. http://doi.org/10.1061/(ASCE)EE.1943–7870.0001709
8. Han M, Jafarikojour M, Mohseni M (2021) The impact of chloride and chlorine radical on nitrite formation during vacuum UV photolysis of water. Sci Total Environ 760: 143325. http://doi.org/10.1016/j.scitotenv.2020.143325
9. Hong J, Li W, Lin B, Zhan M, Liu C, Chen B (2013) Deciphering the effect of salinity on the performance of submerged membrane bioreactor for aquaculture of bacterial community. Desalination 316: 23–30. http://doi.org/10.1016/j.desal.2013.01.015
10. Jung D, Kruse A (2017) Evaluation of Arrhenius–type overall kinetic equations for hydrothermal c arbonization. J Anal appl Pyrol 127: 286–291. http://doi.org/10.1016/j.jaap.2017.07.023
11. Lee J, Park H, Choi W (2002) Selective photocatalytic oxidation of NH_3 to N_2 on platinized TiO_2 in Water. Environ Sci Technol 36: 5462–5468. http://doi.org/10.1021/es025930s
12. Levchuk I, Homola T, Moreno–Andrés J, Rueda–Márquez JJ, Dzik P, Moríñigo MÁ, Sillanpää M, Manzano MA, Vahala R (2019) Solar photocatalytic disinfection using ink–jet printed composite TiO_2/SiO_2 thin films on flexible substrate: Applicability to drinking and marine water. Sol Energy 191: 518–529. http://doi.org/10.1016/j.solener.2019.09.038
13. Li T, Guo Z, She Z, Zhao Y, Guo L, Gao M, Jin C, Ji J (2020) Comparison of the effects of salinity on microbial community structures and functions in sequencing batch reactors with and without carriers. Bioproc Biosyst Eng 43: 2175–2188. http://doi.org/10.1007/s00449–020–02403–8
14. Liou S, Dodd MC (2021) Evaluation of hydroxyl radical and reactive chlorine species generation from the superoxide/hypochlorous acid reaction as the basis for a novel advanced oxidation process. Water Res, 117142. http://doi.org/10.1016/j.watres.2021.117142
15. Mingmongkol Y, Trung Tri Trinh D, Channei D, Khanitchaidecha W, Nakaruk A (2021) Decomposition of dye pigment via photocatalysis process using CuO–TiO_2 nanocomposite. Materials Today: Proceedings. http://doi.org/10.1016/j.matpr.2021.03.330
16. Peng C, Chai L, Tang C, Min X, Song Y, Duan C, Yu C (2017) Study on the mechanism of copper–ammonia complex decomposition in struvite formation process and enhanced ammonia and copper removal. J Environ Sci–China 51: 222–233. http://doi.org/10.1016/j.jes.2016.06.020
17. RigoniStern S, Szpyrkowicz L, ZilioGrandi F (1996) Treatment of silk and Lycra printing wastewaters with the objective of water reuse. Water Sci Technol 33: 95–104. http://doi.org/10.1016/0273–1223(96)00266–1
18. She Z, Zhao L, Zhang X, Jin C, Guo L, Yang S, Zhao Y, Gao M (2016) Partial nitrification and denitrification in a sequencing batch reactor treating high–salinity wastewater. Chem Eng J 288: 207–215. http://doi.org/10.1016/j.cej.2015.11.102

19. Song M, Song B, Meng F, Chen D, Sun F, Wei Y (2019) Incorporation of humic acid into biomass derived carbon for enhanced adsorption of phenol. Sci Rep 9: 19931. http://doi.org/10.1038/s41598−019−56425−8
20. Song W, Li J, Fu C, Wang Z, Zhang X, Yang J, Hogland W, Gao L (2019) Kinetics and pathway of atrazine degradation by a novel method: Persulfate coupled with dithionite. Chem Eng J 373: 803−813. http://doi.org/10.1016/j.cej.2019.05.110
21. Takata S, Sakamoto M, Yamamoto T, Tamazaki F, Shiratori Y (2019) Study on Ni−(Ce,Zr,M)O_2−δ anode for direct internal reforming SOFC fueled by biogas. ECS Transactions 91: 1993−2000. http://doi.org/10.1149/09101.1993ecst
22. Wang H, Su Y, Zhao H, Yu H, Chen S, Zhang Y, Quan X (2014) Photocatalytic oxidation of aqueous ammonia using atomic single layer graphitic−C_3N_4. Environ Sci Technol 48: 11984−90. http://doi.org/10.1021/es503073z
23. Wang J, Yan H, Xin K, Tao T (2019) Iron stability on the inner wall of prepared polyethylene drinking pipe: Effects of multi−water quality factors. Sci Total Environ 658: 1006−1012. http://doi.org/10.1016/j.scitotenv.2018.12.127
24. Wang L, Lan X, Peng W, Wang Z (2021) Uncertainty and misinterpretation over identification, quantification and transformation of reactive species generated in catalytic oxidation processes: A review. J Hazard Mater 408: 124436. http://doi.org/10.1016/j.jhazmat.2020.124436
25. Wang S, Wu J, Lu X, Xu W, Gong Q, Ding J, Dan B, Xie P (2019) Removal of acetaminophen in the Fe^{2+}/persulfate system: Kinetic model and degradation pathways. Chem Eng J 358: 1091−1100. http://doi.org/10.1016/j.cej.2018.09.145
26. Yang Q, Kocherginsky NM (2007) Copper removal from ammoniacal wastewater through a hollow fiber supported liquid membrane system: Modeling and experimental verification. J Membrane Sci 297: 121−129. http://doi.org/10.1016/j.memsci.2007.03.036
27. Yao F, Fu W, Ge X, Wang L, Wang J, Zhong W (2020) Preparation and characterization of a copper phosphotungstate/titanium dioxide (Cu−$H_3PW_{12}O_{40}$/TiO_2) composite and the photocatalytic oxidation of high−concentration ammonia nitrogen. Sci Total Environ 727: 138425. http://doi.org/10.1016/j.scitotenv.2020.138425
28. Zeng Z, Zhang M, Kang D, Li Y, Yu T, Li W, Xu D, Zhang W, Shan S, Zheng P (2019) Enhanced anaerobic treatment of swine wastewater with exogenous granular sludge: Performance and mechanism. Sci Total Environ 697. http://doi.org/10.1016/j.scitotenv.2020.138425
29. Zheng L, Chen Y, Zhou S, Chen Y, Wang X, Wang X, Zhang L, Chen Z (2020) Nitrogen removal for liquid−ammonia mercerization wastewater via partial nitritation/anammox based on zeolite sequencing batch reactor. Water−Sui 12: 2234. http://doi.org/10.3390/w12082234
30. Zhou Q, Yin H, Wang A, Si Y (2019) Preparation of hollow B−SiO_2@TiO_2 composites and their p hotocatalytic performances for degradation of ammonia−nitrogen and green algae in aqueous solution. Chinese J Chem eng 27: 2535−2543. http://doi.org/10.1016/j.cjche.2019.01.036

Figures

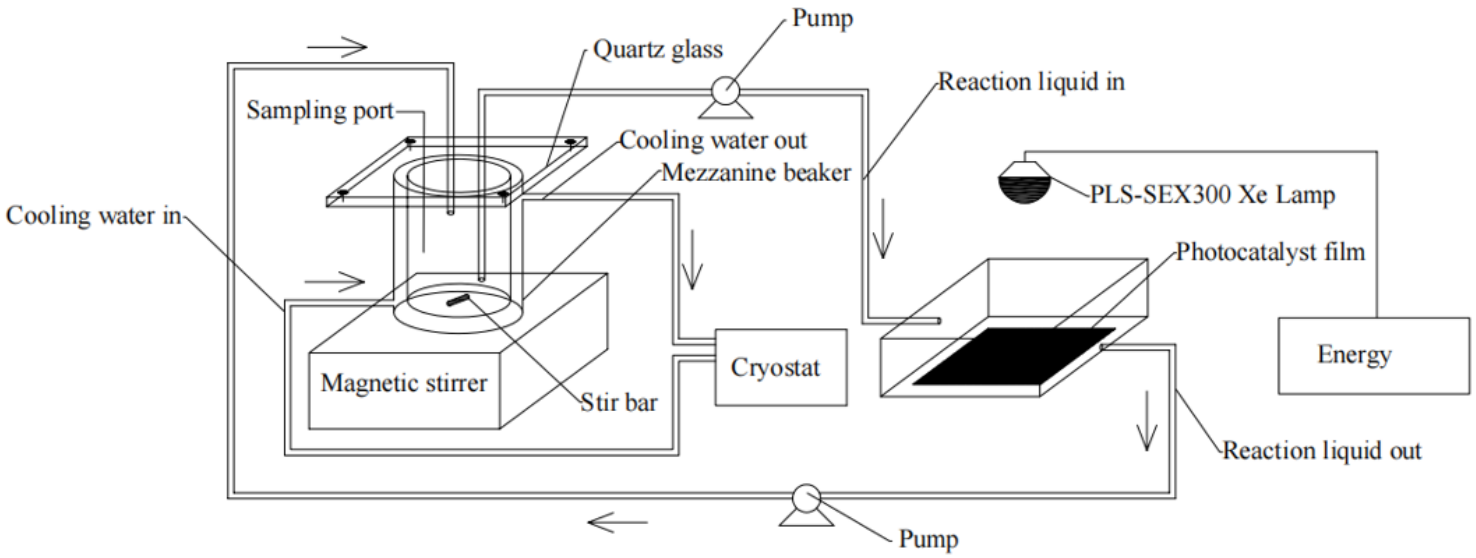

Figure 1

The experimental setup for evaluating photocatalyst film

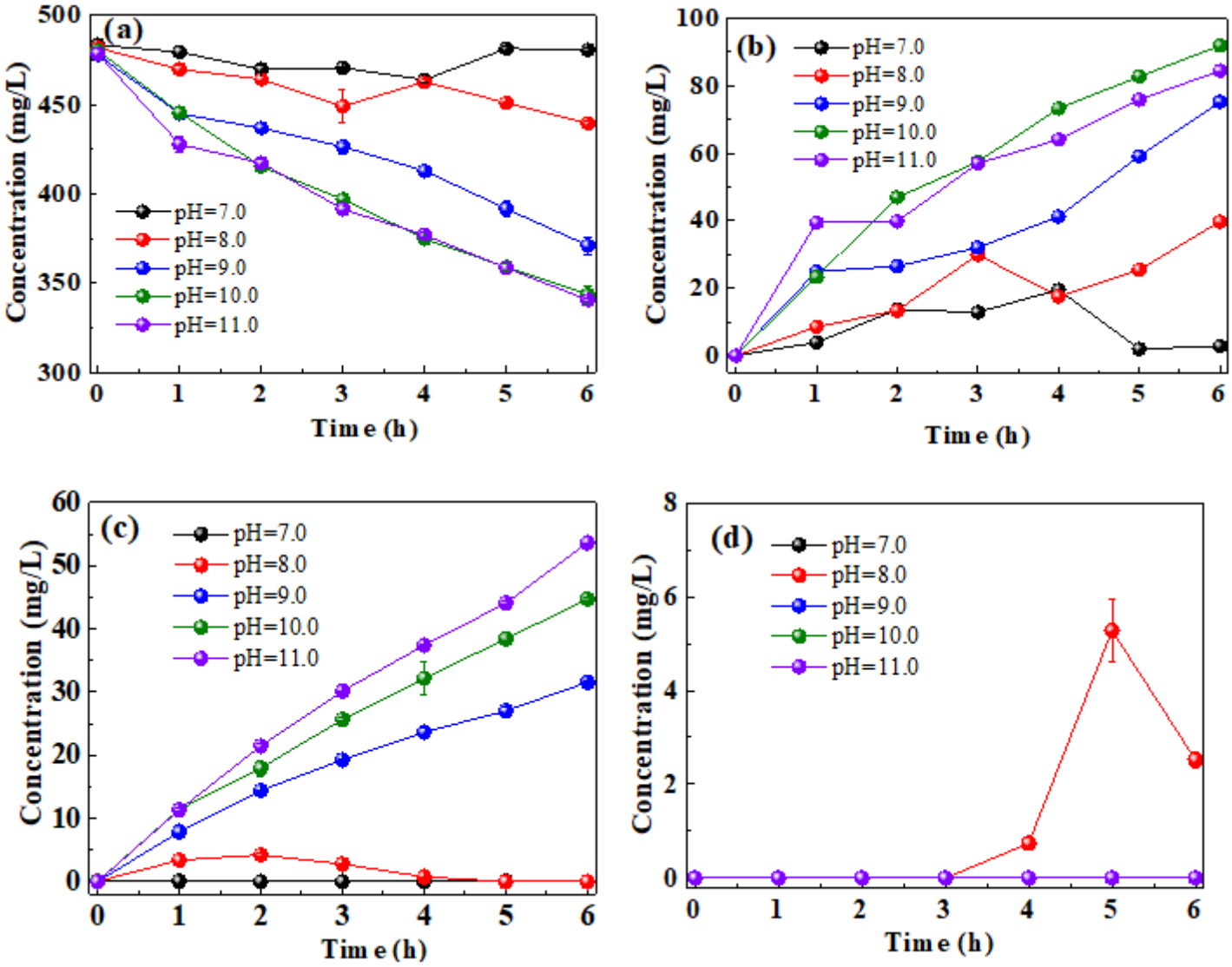

Figure 2

(a) Photocatalytic conversion of ammonia nitrogen in aqueous solution by Cu/TiO2 (0.5 g/L) with different initial pH; (b) production of gaseous–N species; (c) production of nitrite nitrogen; (d) production of nitrate nitrogen

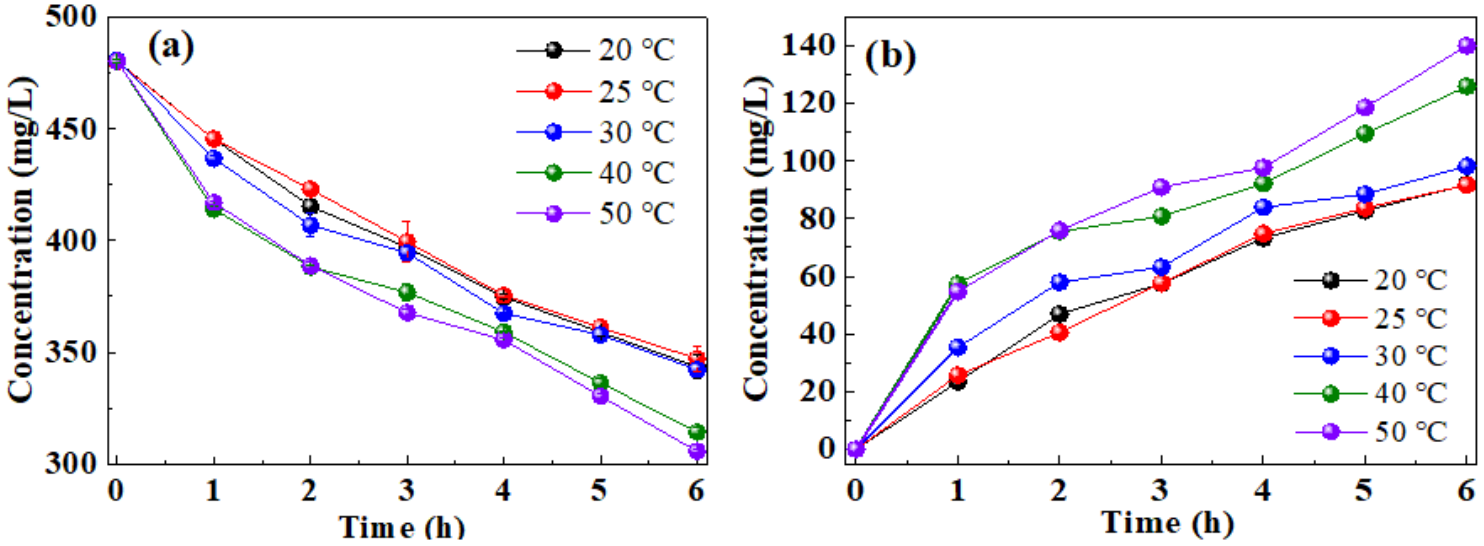

Figure 3

Photocatalytic conversion of ammonia nitrogen in aqueous solution at pH = 10 by Cu/TiO2 (0.5 g/L) with different temperature; (b) production of gaseous−N species

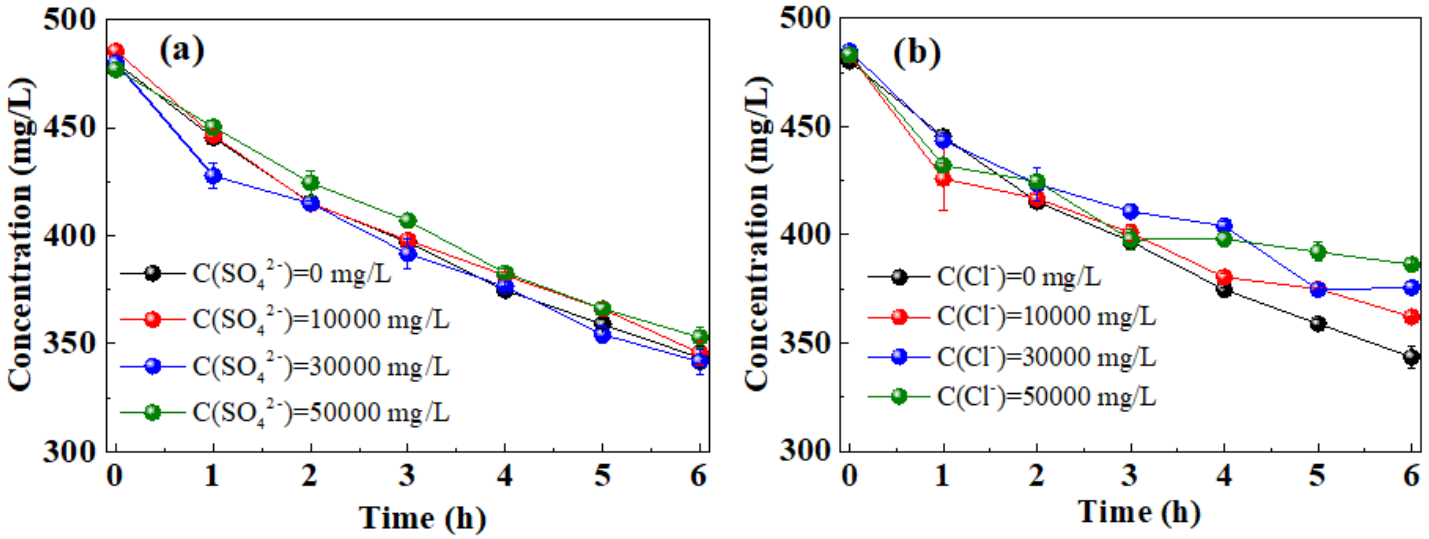

Figure 4

Photocatalytic conversion of ammonia nitrogen in aqueous solution by Cu/TiO2 in the presence of different concentration of (a) SO42− and (b) Cl−

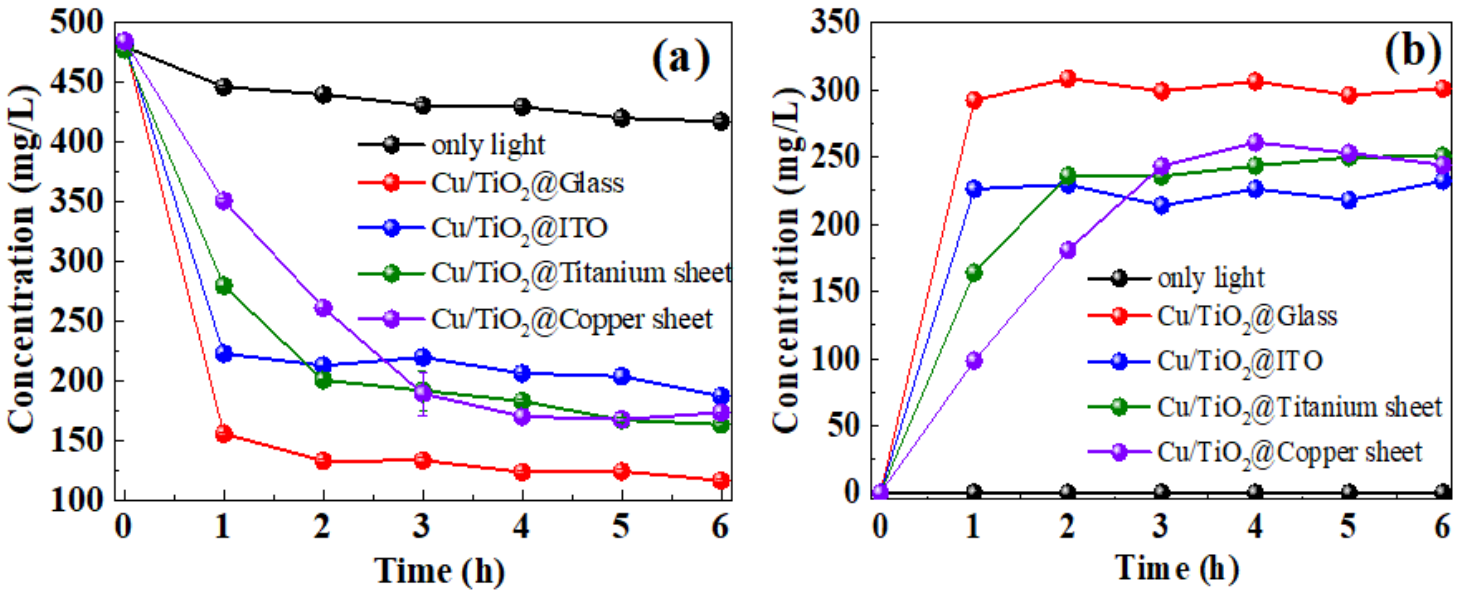

Figure 5

(a) Photocatalytic conversion of ammonia nitrogen in aqueous solution by Cu/TiO2 films with different supports; (b) Production of gaseous−N species during photocatalytic oxidation.

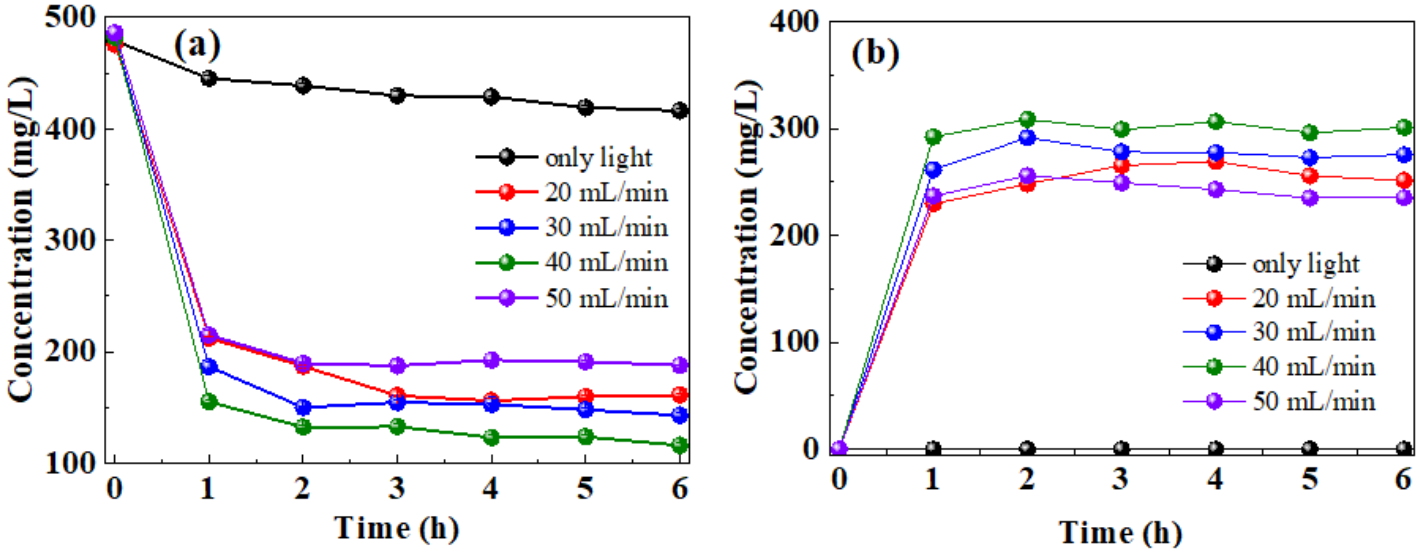

Figure 6

(a) Photocatalytic conversion of ammonia nitrogen in aqueous solution by Cu/TiO2@Glass with different flow rates; (b) production of gaseous−N species during photocatalytic oxidation.

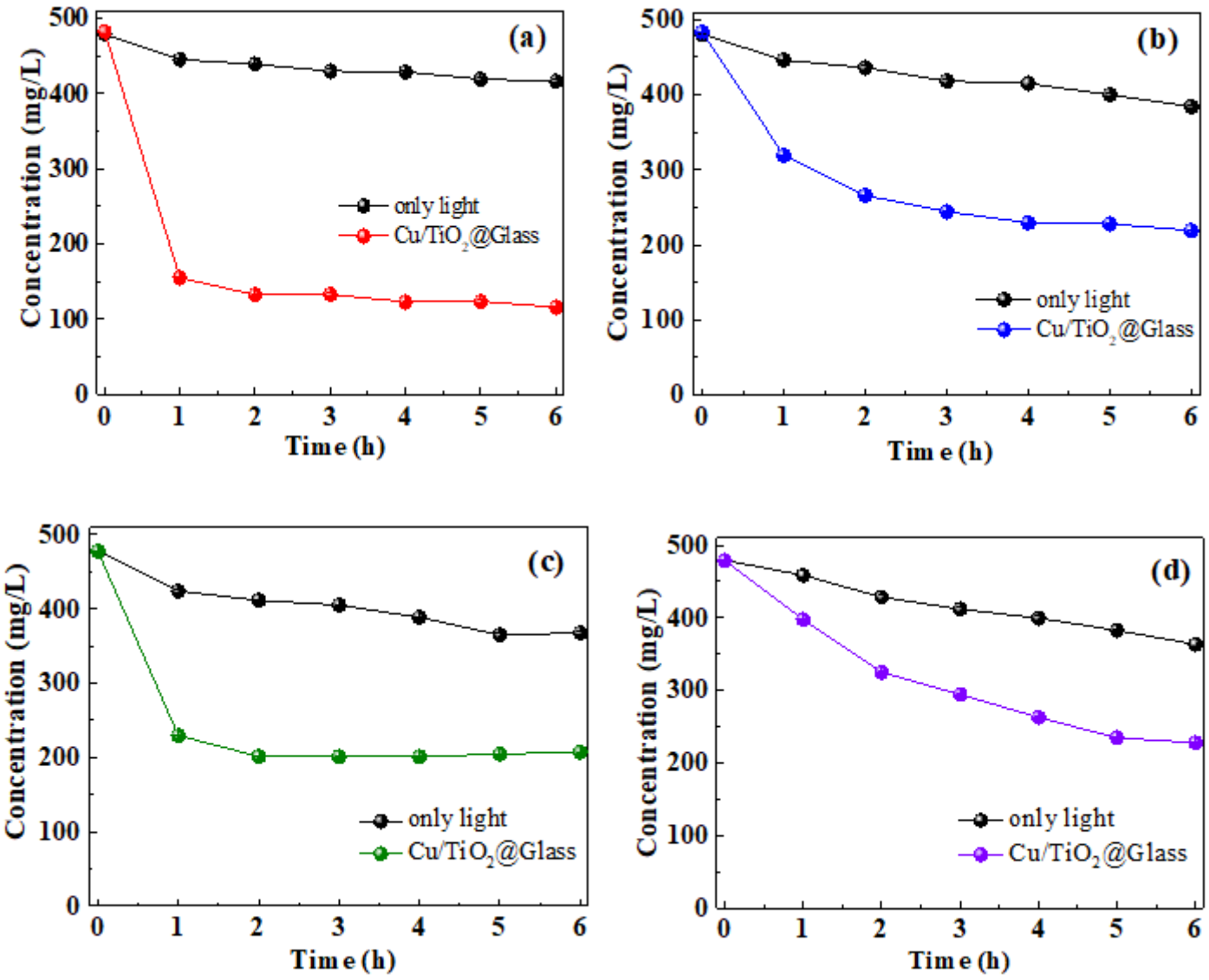

Figure 7

Photocatalytic degradation of ammonia nitrogen (500 mg/L) in different aqueous solution by Cu/TiO2@Glass under the irradiation of Xe lamp. (a) control experiment; (b) high salinity ammonia nitrogen wastewater; (c) copper–ammonia complex wastewater; (d) liquid–ammonia mercerization wastewater.

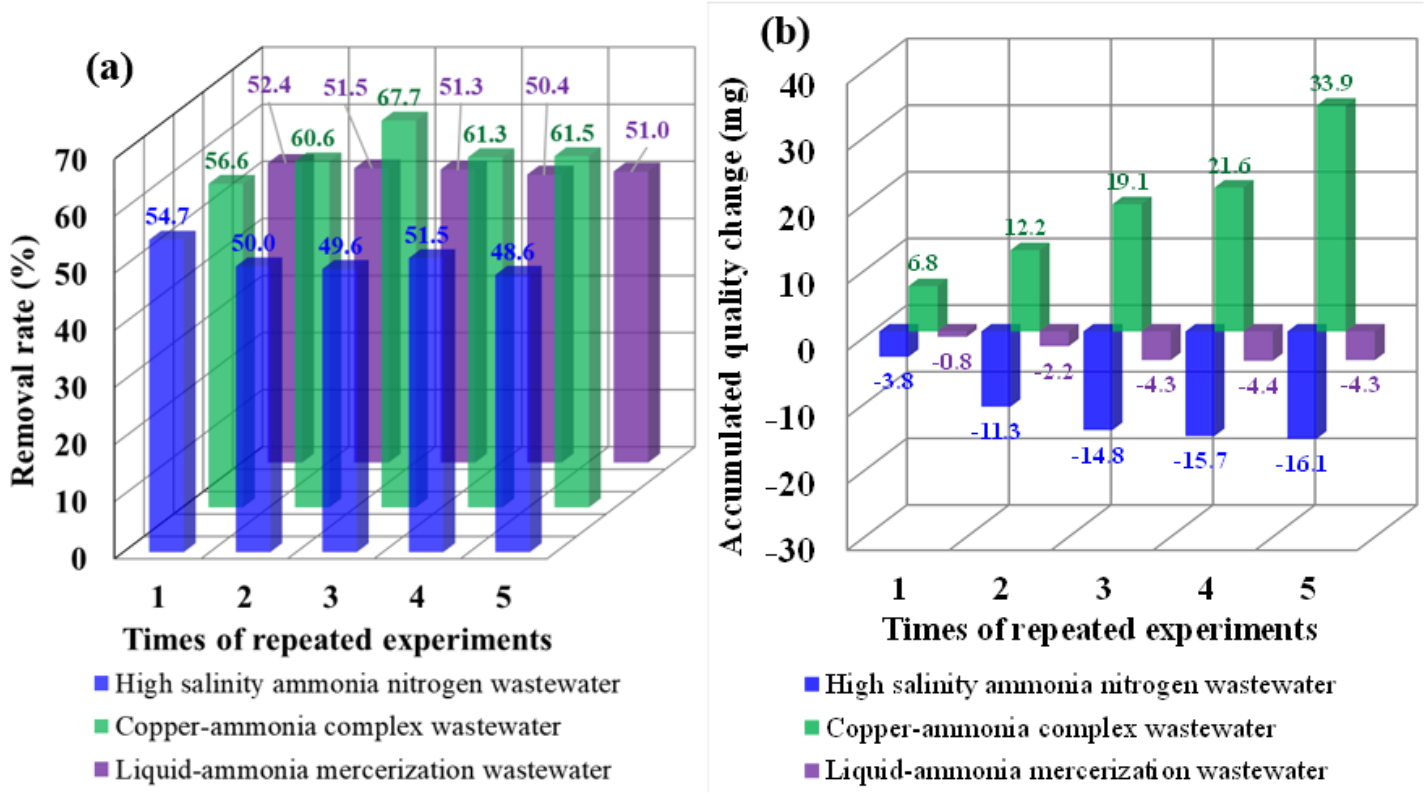

Figure 8

(a) The photocatalytic removal rate of ammonia nitrogen in three types of wastewater by Cu/TiO2@Glass; (b) accumulated mass change of catalyst film after multiple experiments

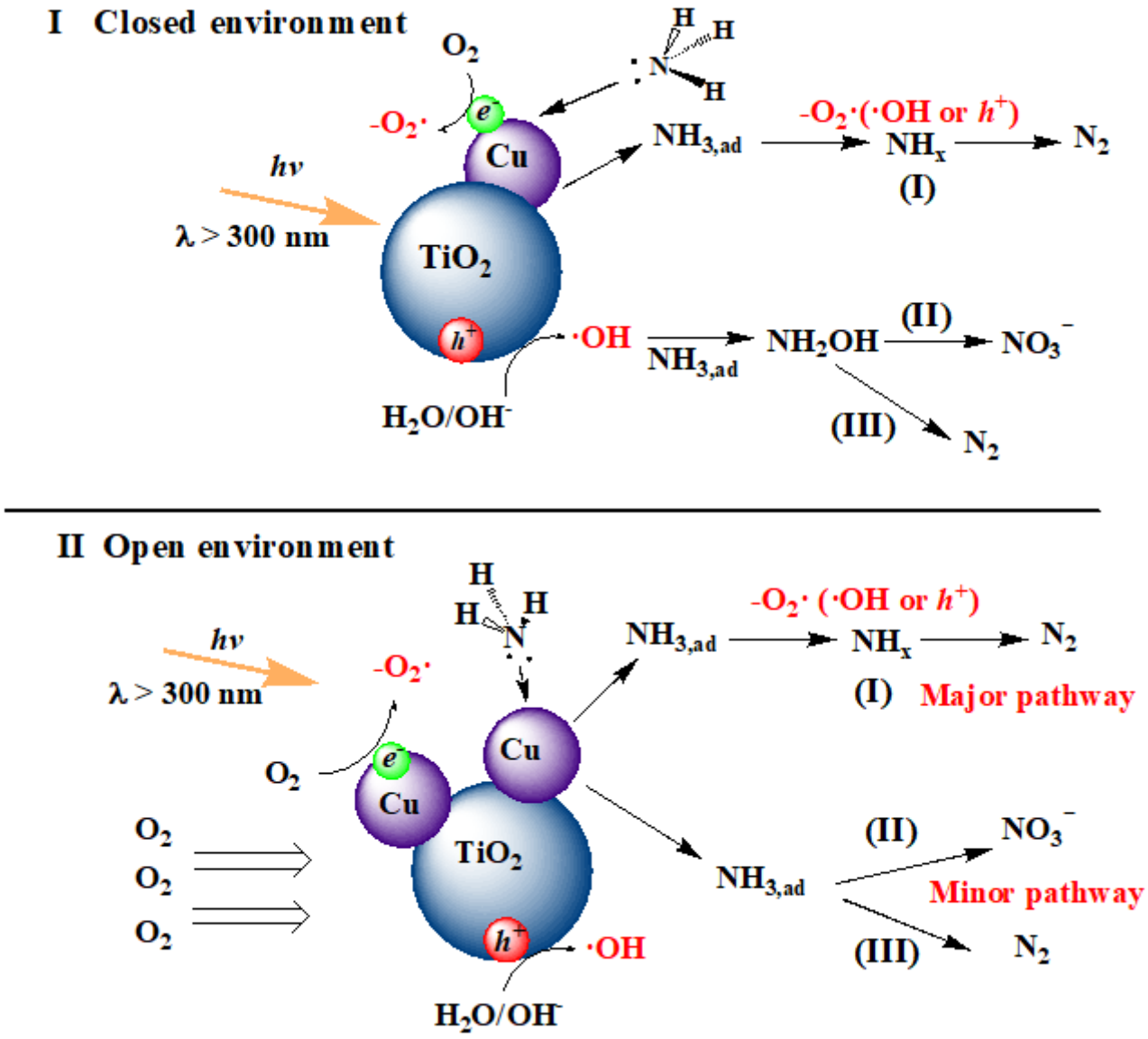

Figure 9

Illustrations of possible oxidation pathways in photocatalytic oxidation of ammonia by Cu/TiO2 powder in the closed system and by Cu/TiO2 film in the open system.

Supplementary Files

This is a list of supplementary files associated with this preprint. Click to download.

- msSI063001.docx